

## **Glass Wool Supported Ruthenium Complexes: Versatile, Recyclable Heterogeneous Photoredox Catalysts**

*Rodolfo I. Teixeira,<sup>1,2</sup> Nanci C. De Lucas,<sup>2\*</sup> Simon J. Garden,<sup>2</sup> Anabel E. Lanterna,<sup>1</sup> Juan C. Scaiano.<sup>1\*</sup>*

<sup>1</sup>Department of Chemistry and Biomolecular Science and Centre for Advanced Materials Research (CAMaR),  
University of Ottawa, 10 Marie Curie, Ottawa, ON K1N 6N5, Canada.

<sup>2</sup>Instituto de Química, Universidade Federal do Rio de Janeiro, 149 Athos da Silveira Ramos Avenue, Cidade  
Universitária, Rio de Janeiro, RJ, 21949-909, Brazil.

### **Corresponding authors:**

JCS: [titoscaiano@mac.com](mailto:titoscaiano@mac.com)

NCDL: [nancicl@iq.ufrj.br](mailto:nancicl@iq.ufrj.br)

## Table of content

General Information	5
Materials	5
Instrumentation	5
Figure S1. General appearance of functionalized glass wool materials.	7
Figure S2. Examples of the macroscopic appearance of modified glass wool under ambient-light or UV irradiation.	7
Materials Characterization	8
Diffuse Reflectance Spectroscopy	8
Figure S3. Diffuse reflectance spectra of (A) GW@AQ, (B) GW@EY, (C) GW@RB and (D) GW*.	8
Figure S4. Diffuse reflectance spectrum of GW@RuB <sub>Ads</sub> .	8
Fluorescence Spectroscopy	9
Figure S5. Fluorescence spectra of GW@EY ( <i>left</i> ) and GW@RB ( <i>right</i> ).	9
Figure S6. Fluorescence spectra of GW@RuB (black), GW@Ru-Ads (blue) and GW* (red).	9
X-ray Photoelectron Spectroscopy	10
Figure S7. XPS survey spectrum of GW*.	10
Figure S8. XPS survey spectrum of GW@RuB.	10
Figure S9. XPS survey spectrum of GW@RuP.	11
Figure S10. XPS survey spectrum of GW@AQ.	11
Figure S11. XPS survey spectrum of GW@RB.	12
Figure S12. XPS survey spectrum of GW@EY.	12
Figure S13. N 1s HR-XPS spectra of (A) GW*, (B) GW@RuB, and (C) GW@RuP.	13
Figure S14. High-Resolution XPS spectra of GW@AQ.	14
Figure S15. High-Resolution XPS spectra of GW@RB.	14

Figure S16. High-Resolution XPS spectra of GW@EY.	15
NMR Spectroscopy	16
Figure S17. <sup>1</sup> H NMR spectrum of phenol obtained by oxidative hydroxylation of phenylboronic acid. *maleic acid (7.4 mg).	16
Figure S18. <sup>1</sup> H NMR spectrum of 4-fluorophenol obtained by oxidative hydroxylation of 4- fluorophenylboronic acid. *maleic acid (9.3 mg).	17
Figure S19. <sup>1</sup> H NMR spectrum of 4-chlorophenol obtained by oxidative hydroxylation of 4- chlorophenylboronic acid. *maleic acid (9.2 mg).	17
Figure S20. <sup>1</sup> H NMR spectrum of 4-methoxyphenol obtained by oxidative hydroxylation of 4-methoxy phenylboronic acid. *maleic acid (10.2 mg).	18
Figure S21. <sup>1</sup> H NMR spectrum of 4-(trifluoromethyl)phenol obtained by oxidative hydroxylation of 4- (trifluoromethyl)phenylboronic acid. *maleic acid (36 mg).	18
Figure S22. <sup>1</sup> H NMR spectrum of RuB.	19
Figure S23. <sup>13</sup> C NMR spectrum of RuB.	19
Figure S24. <sup>1</sup> H NMR spectrum of RuP.	20
ESI-HRMS	21
Figure S25. ESI-HRMS of RuB.	21
Figure S26. ESI-HRMS of RuP.	21
Additional Results	22
Figure S27. Absorption spectra of Ru-complexes versus MB.	22
Figure S28. Emission spectrum of the reaction mixture of the hydroxylation of phenylboronic acid 6h after irradiation (blue LED) using GW@RuB as catalyst. Notice there is no evidence of RuB leaching during reaction (cft. inset: Emission spectrum of GW@RuB).	22
Figure S29. Kinetics of the photooxidation of a 100 μM DMA solution using GW@RuB as catalyst. Solvent: MeCN.	23
Figure S30. <sup>1</sup> H NMR spectra of DMA before (black) and after 6 h of (blue) blue LED irradiation using GW@RuB.	24

Figure S31. Decay of the DMA emission intensity versus time of irradiation (Blue LED) using GW@RuB as catalyst. General Procedure: 15 min irradiation of 5 mL of a DMA solution in the presence of 5 mg of GW@RuB. Filtration to remove the catalyst and further 15 min irradiation of the solution (grey area). Resubmission of catalyst into the solution and another 15 min irradiation cycle. Notice negligible conversion when the catalyst is taken out of the solution. 25

Figure S32. Emission spectrum of the reaction mixture of DMA oxidation after 2 h of blue LED irradiation using GW@RuP as catalyst. Notice there is no evidence of RuB leaching during reaction (*cft.* inset: Emission spectrum of GW@RuP). 25

Figure S33. <sup>1</sup>H NMR spectra of 2-ethylfuran before (red), and after 3h (green) or 6h (blue) of blue LED irradiation using GW@RuB as catalyst. 26

Excitation Sources 27

Figure S34. Emission spectra of (*top*) blue LED –working intensity: 1235 W/m<sup>2</sup>; (*middle*) green LED –working intensity: 855 W/m<sup>2</sup>; (*bottom*) white light LED –working intensity: 2385 W/m<sup>2</sup>. 27

## General Information

### *Materials*

All chemicals used in this work are commercially available unless otherwise noted, and were used as received.

### *Instrumentation*

UV-Vis spectroscopy was carried out in an UV-Visible spectrophotometer Varian Cary 50 Bio using 1x1 cm quartz cuvettes. Diffuse reflectance spectroscopy was performed in an Agilent Cary 7000 spectrophotometer using the UV-Vis-NIR Diffuse Reflectance Accessory.

Fluorescence spectroscopy was carried out in a Horiba/PTI spectrofluorimeter with a Xenon lamp, an LPS-220 Lamp Power Supply, a MD-5020 motor driver and a SC-500 shutter controller. Solid-state emission spectra were acquired in a Perkin Elmer Luminescence Spectrometer LS50 by using a front-face support and quartz disc as sample holders.

Ruthenium loading was determined by Inductively Coupled Plasma Optical Emission 70 Spectrometry (ICP-OES), using an Agilent Vista Pro ICP Emission Spectrometer. The Ru emission line at 240.272 nm was used for quantification. Samples were prepared as duplicates as follow: 100 mg of glass wool samples were added to 1.5 mL of aqua regia (HCl:HNO<sub>3</sub> 3:1) and sonicated for 1 h. Then, the samples were heated to 60 °C for 12 h. The resulted mixture was concentrated to half of the volume. The supernatant was transferred to another tube, and the solid residue was washed 5x with 1 mL miliQ water and the solution attained a final volume of 10 mL. ICP-OES analysis of the reaction mixtures was performed as follows: after 6h of reaction in the presence of 50 mg of GW@RuP (or GW@RuB), the catalyst was filtered off and washed with MeCN (3x1mL) and water (3x1mL). The solvent of the reaction mixture (combined with the washing solvents) was completely dried. The residue was dissolved in 0.5 mL of aqua regia at 80 °C for 6h and then the volume was completed to 5 mL using deionized water.

X-ray Photoelectron Spectroscopy (XPS) analysis was performed on a Kratos Nova AXIS spectrometer equipped with an Al X-ray source. The samples were mounted onto a SEM mount (with the pins cut off) using double-sided adhesive Cu tape. After removing excess glass fibers, the SEM mount was attached to the coated aluminum platen using double-sided adhesive Cu tape and was kept under high vacuum (10<sup>-9</sup> Torr) overnight inside the preparation chamber before they were transferred into the analysis chamber (ultrahigh vacuum, 10<sup>-10</sup> Torr) of the spectrometer. The XPS data were collected using AlK<sub>α</sub> radiation at 1486.69 eV (150 W, 15 kV), charge neutralizer and a delay-line detector (DLD) consisting of three multi-channel plates. Survey spectra were recorded from -5 to 1200 eV at a pass energy of 160 eV

(number of sweeps: 2) using an energy step size of 1 eV and a dwell time of 200 ms. High resolution spectra for O<sub>1s</sub>, N<sub>1s</sub>, C<sub>1s</sub> and Si<sub>2p</sub> were recorded in the appropriate regions at a pass energy of 20 eV (number of sweeps: O<sub>1s</sub>, 5; N<sub>1s</sub>, 15; C<sub>1s</sub>, 10; Si<sub>2p</sub>, 10) using a dwell time of 300 ms and an energy step size of 0.1 eV. The analyzed area on the specimens was about 300 × 700 μm<sup>2</sup> (lens mode: FOV 1) at this position. The incident angle (X-ray source/sample) is the magic angle of 54.74° and the take-off angle (sample/detector) is 90°. All spectra were calibrated at the C 1s signal at 284.8 eV and fittings obtained using a Gaussian 30% Lorentzian and a Shirley baseline.

Gas chromatography coupled to mass spectrometry detection (GC-MS) was carried out by using an Agilent system with a 6890N Network GC System coupled to a 5973 inert Mass Selective Detector. <sup>1</sup>H and <sup>13</sup>C NMR analyses were carried out in a The Bruker Avance II 400MHz NMR spectrometer. HRMS was performed in a BioApex II 70e FTICR spectrometer, Bruker, using the APCI module.

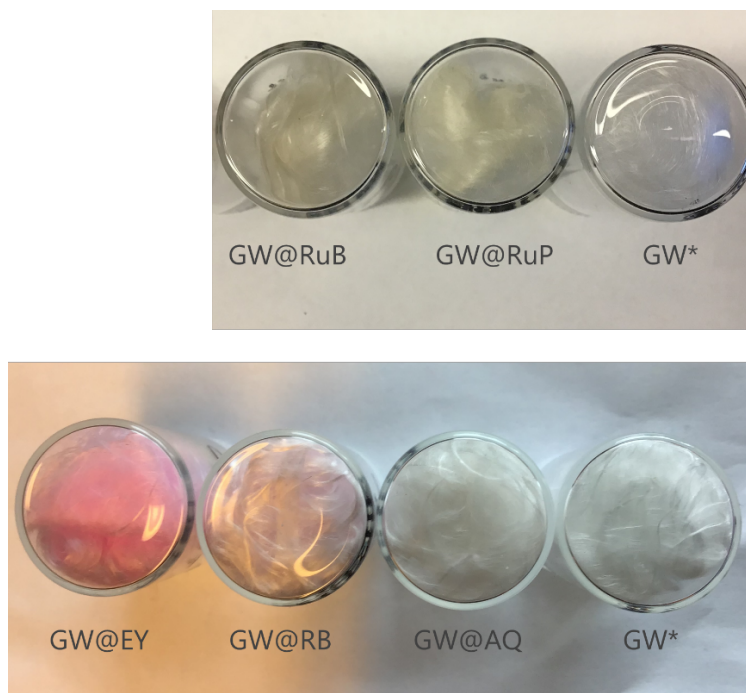


Figure S1. General appearance of functionalized glass wool materials.

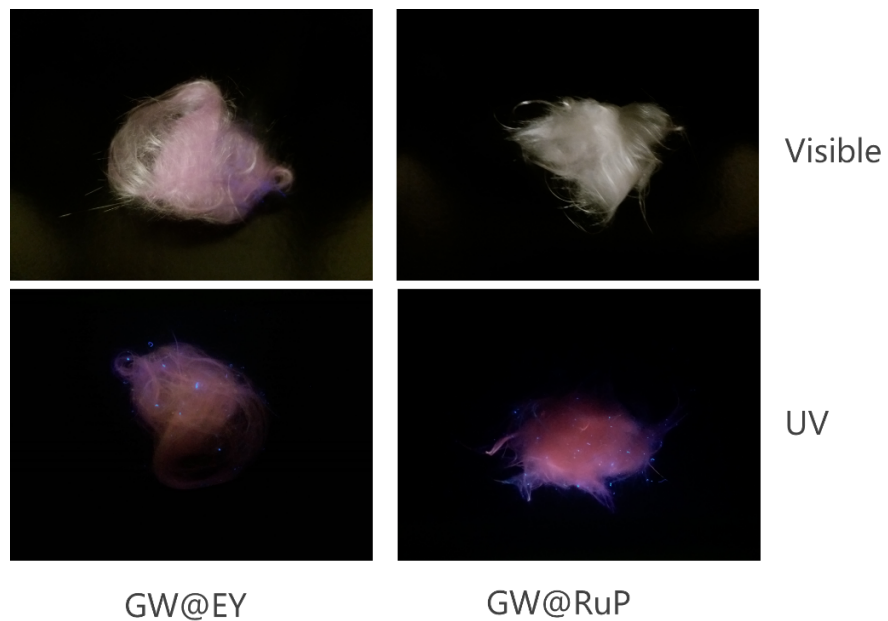


Figure S2. Examples of the macroscopic appearance of modified glass wool under ambient-light or UV irradiation.

## Materials Characterization

### *Diffuse Reflectance Spectroscopy*

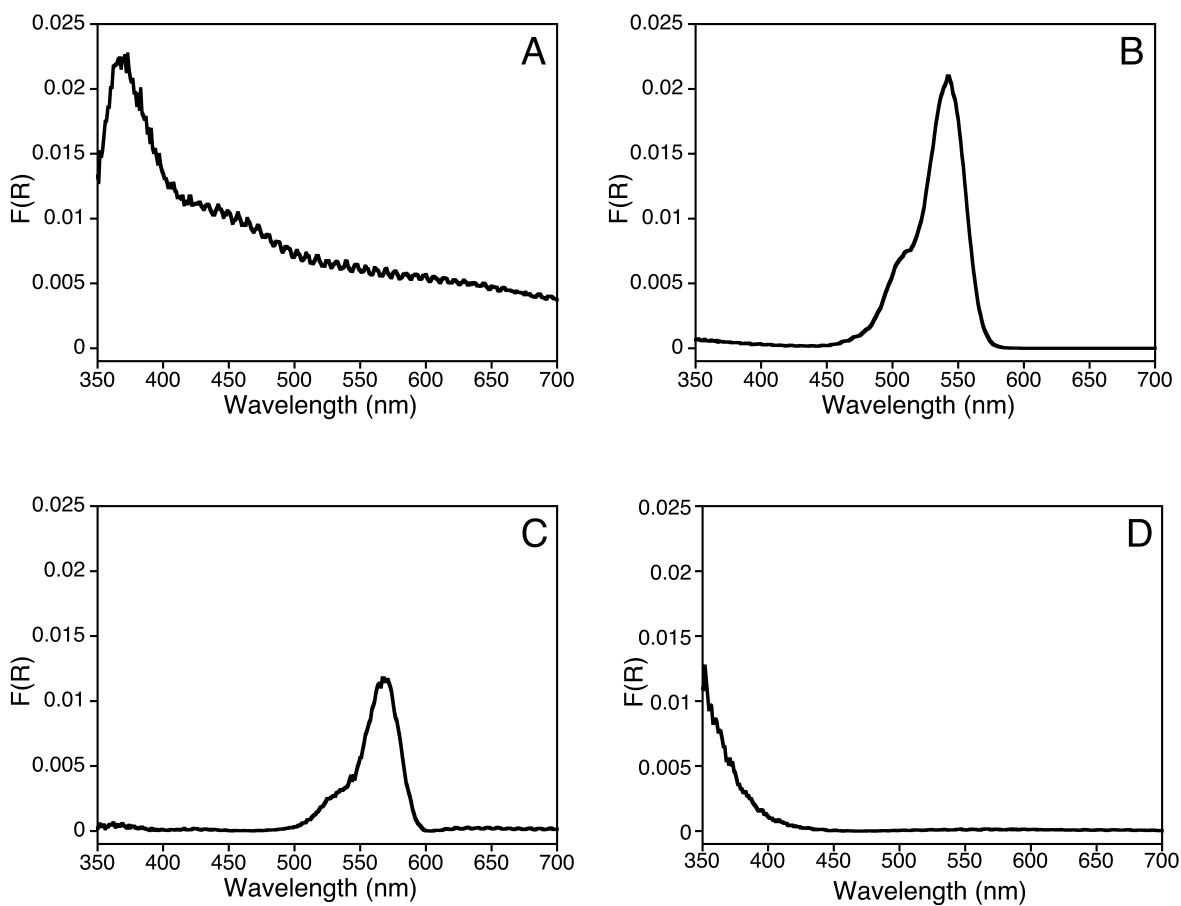


Figure S3. Diffuse reflectance spectra of (A) GW@AQ, (B) GW@EY, (C) GW@RB and (D) GW\*.

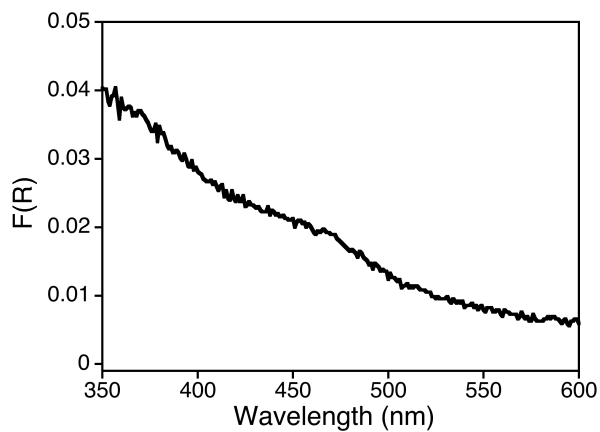


Figure S4. Diffuse reflectance spectrum of GW@RuB<sub>Ads</sub>.

## Fluorescence Spectroscopy

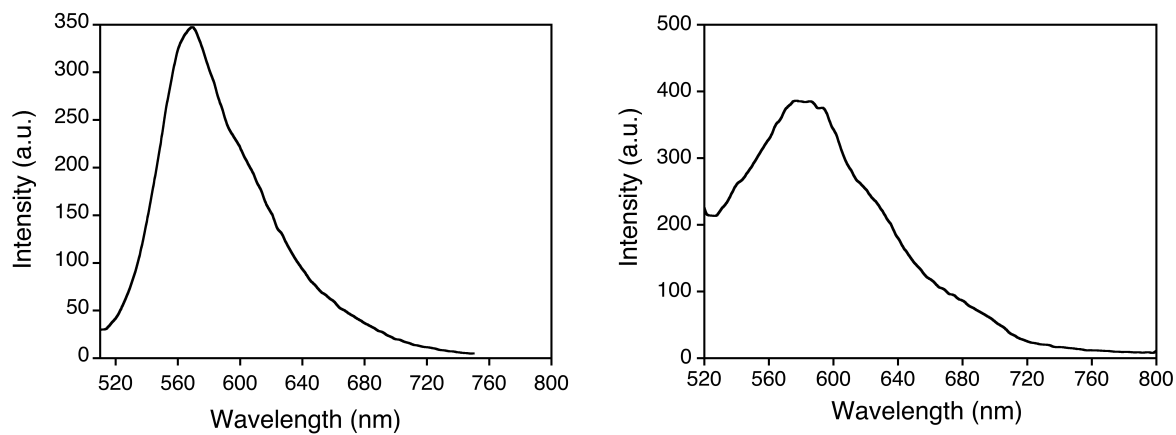


Figure S5. Fluorescence spectra of GW@EY (*left*) and GW@RB (*right*).

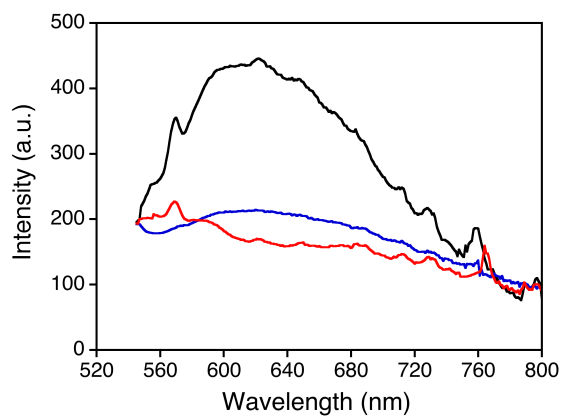


Figure S6. Fluorescence spectra of GW@RuB (black), GW@RuB-Ads (blue) and GW\* (red).

*X-ray Photoelectron Spectroscopy*

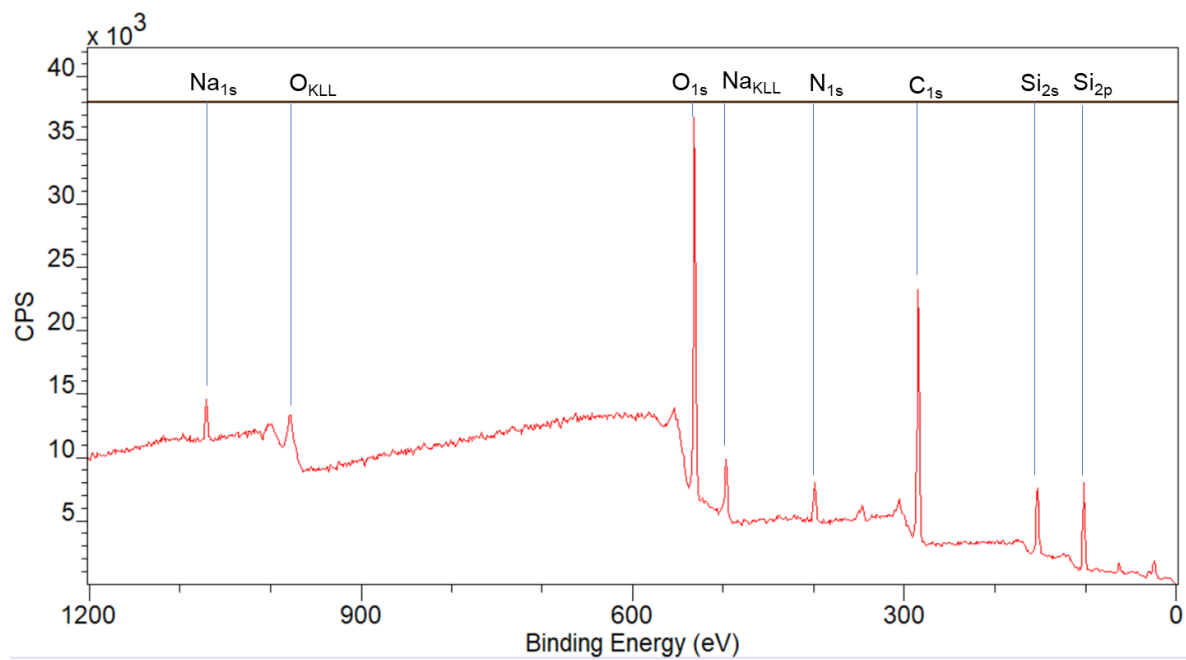


Figure S7. XPS survey spectrum of GW\*.

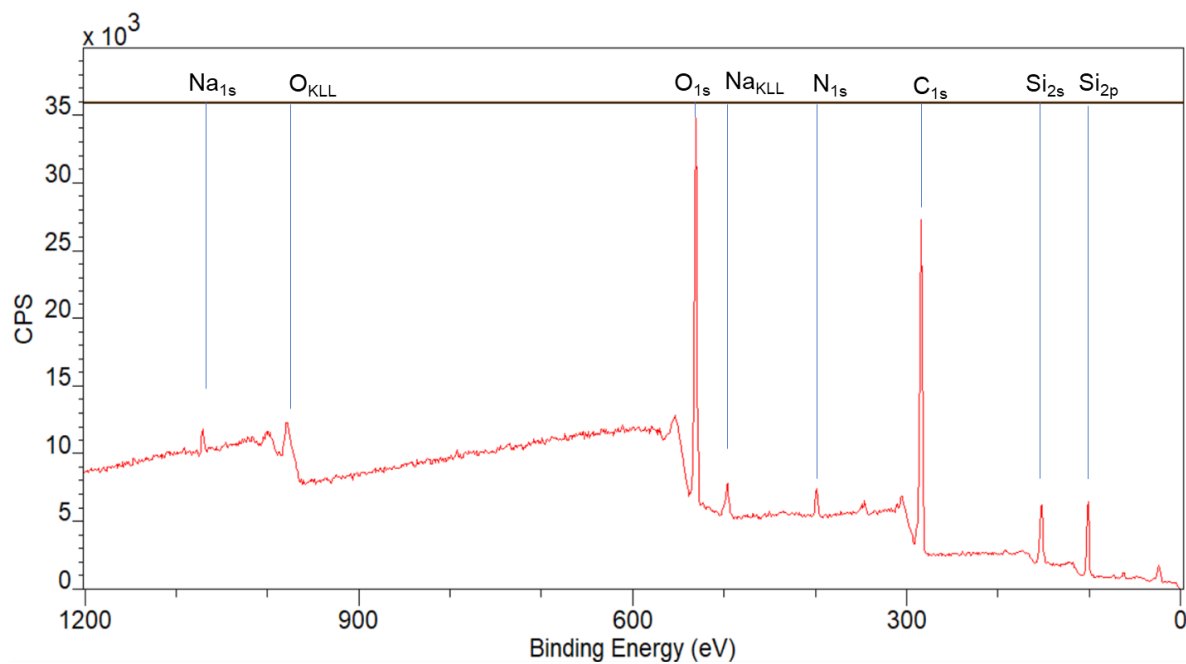


Figure S8. XPS survey spectrum of GW@RuB.

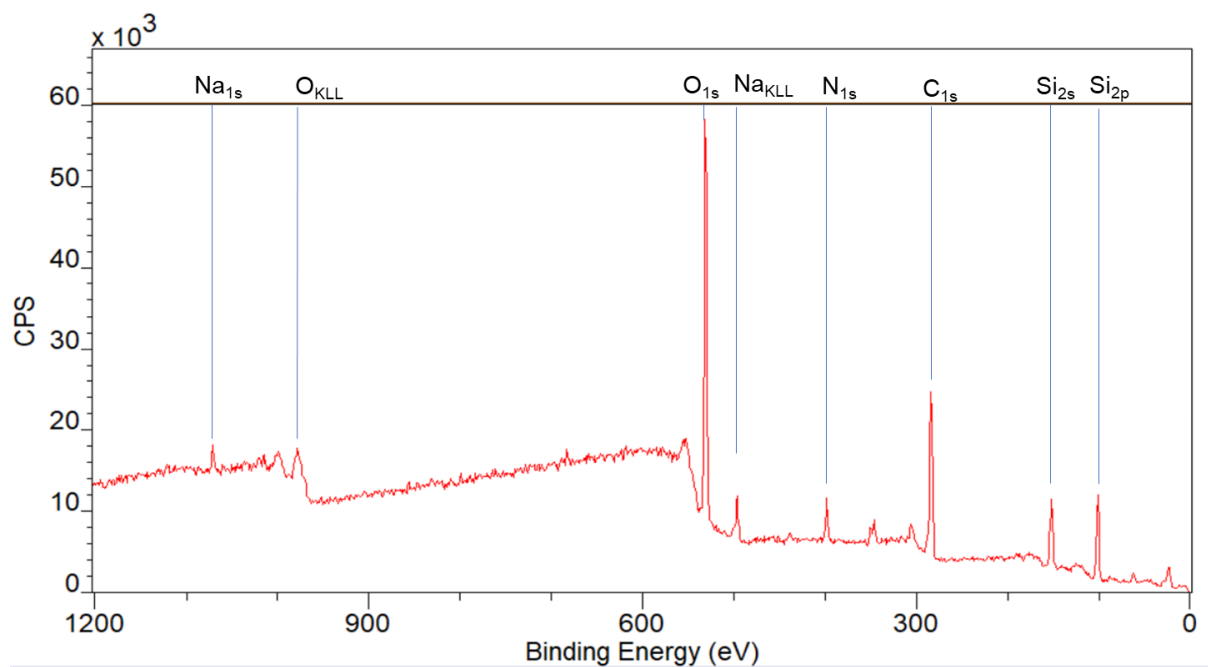


Figure S9. XPS survey spectrum of GW@RuP.

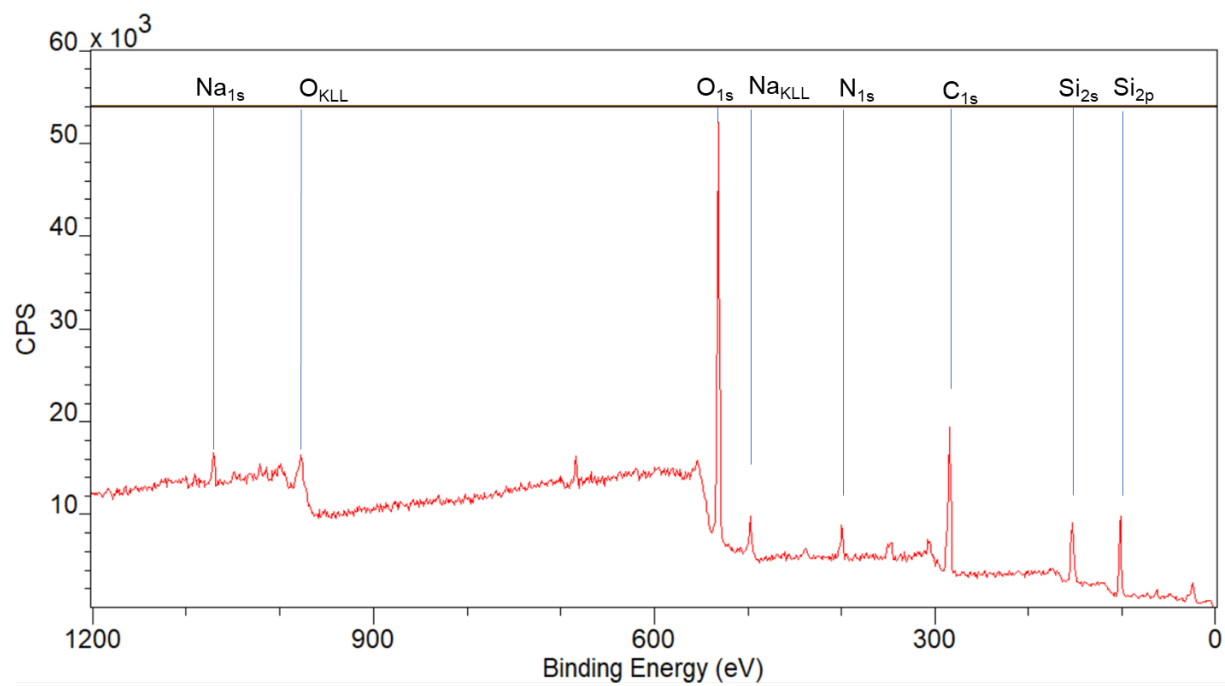


Figure S10. XPS survey spectrum of GW@AQ.

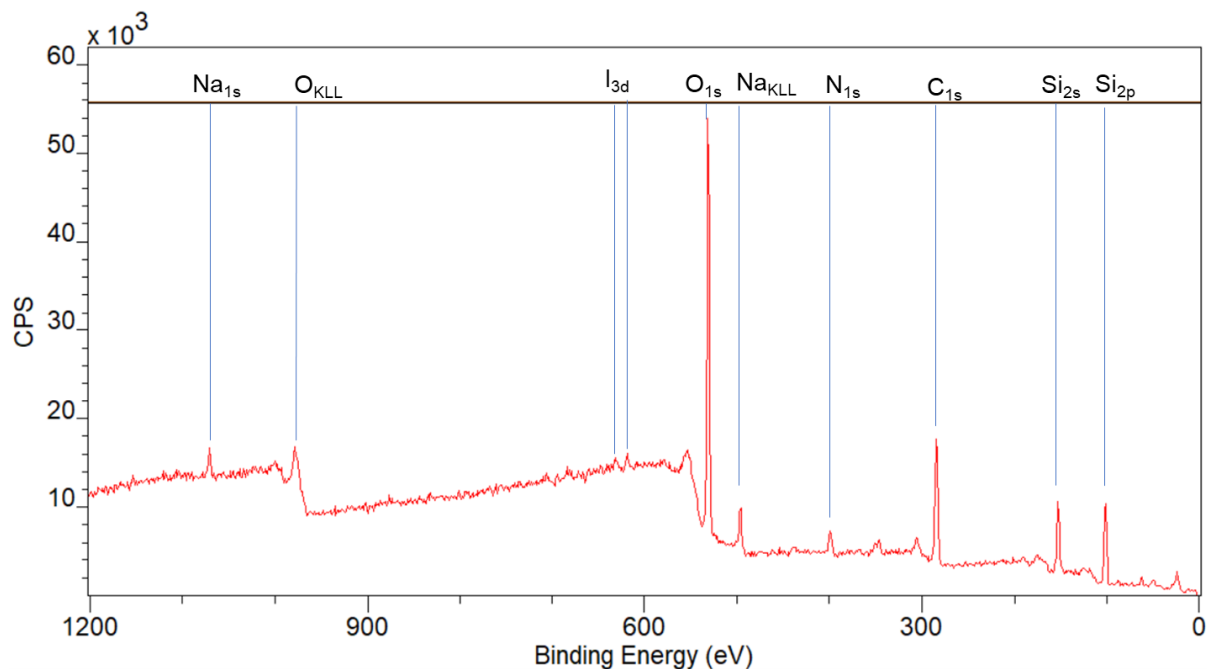


Figure S11. XPS survey spectrum of GW@RB.

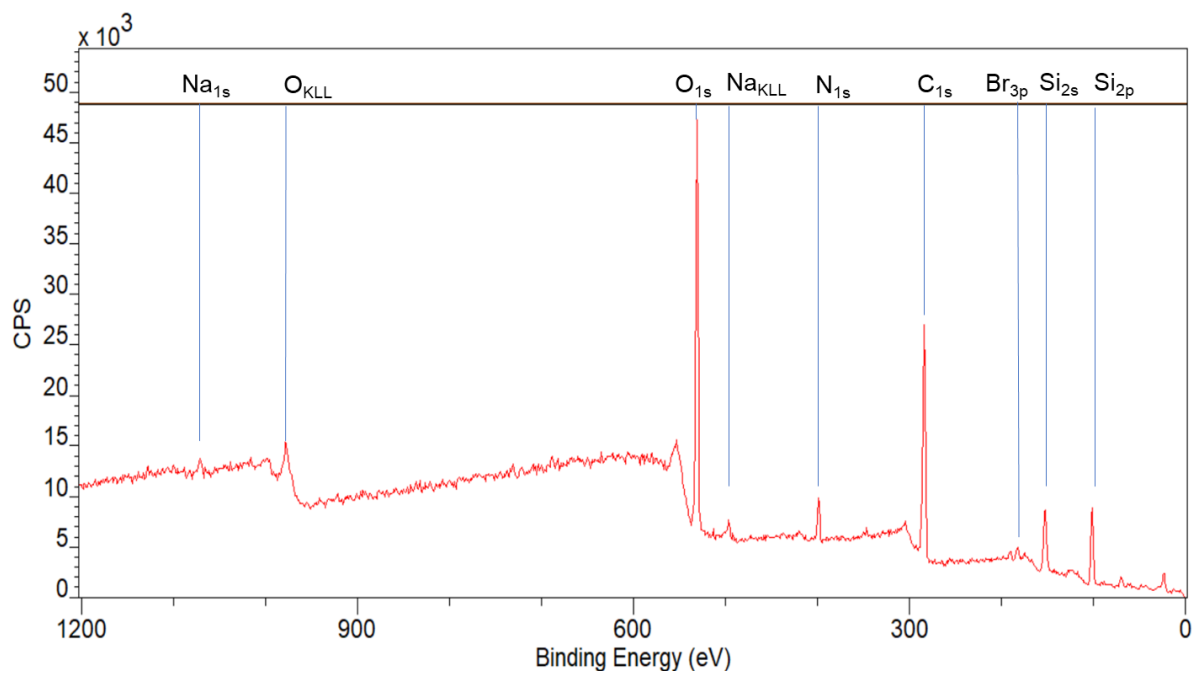


Figure S12. XPS survey spectrum of GW@EY.

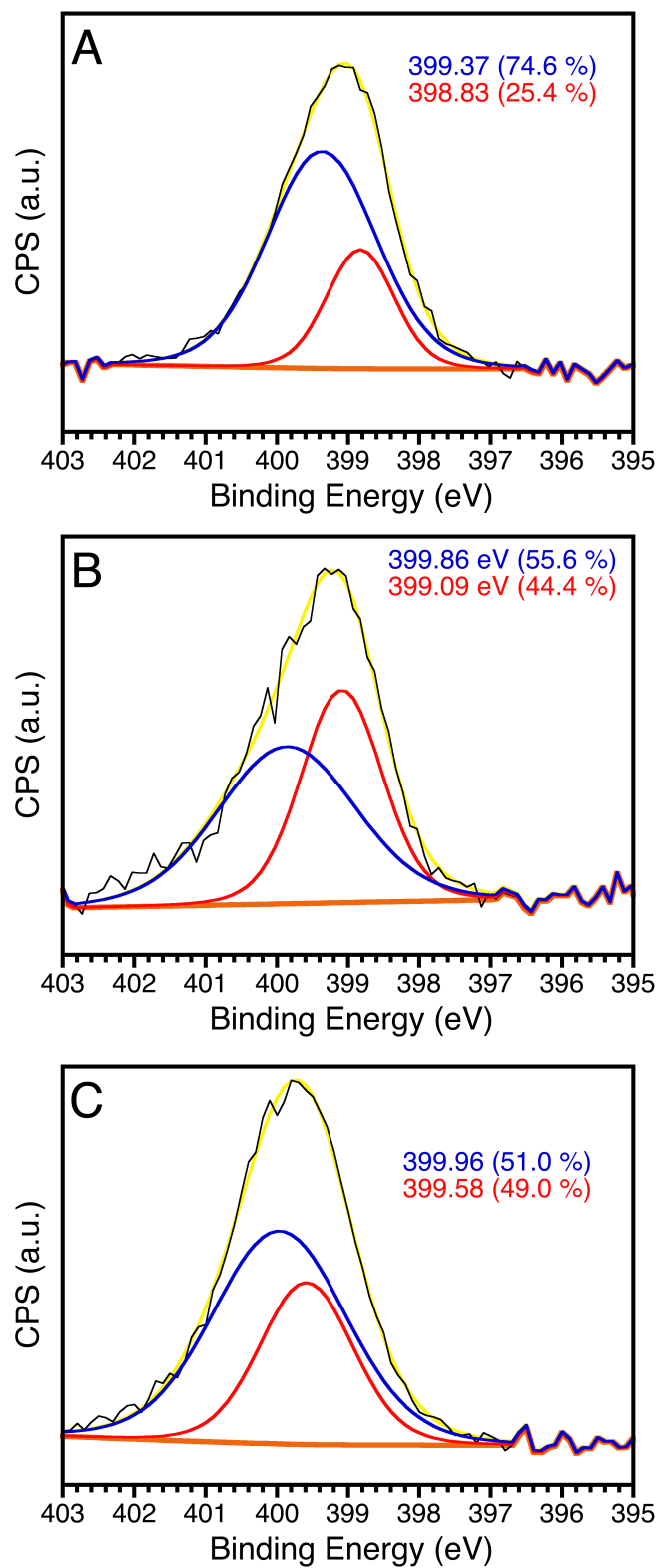


Figure S13. N 1s HR-XPS spectra of (A) GW\*, (B) GW@RuB, and (C) GW@RuP.

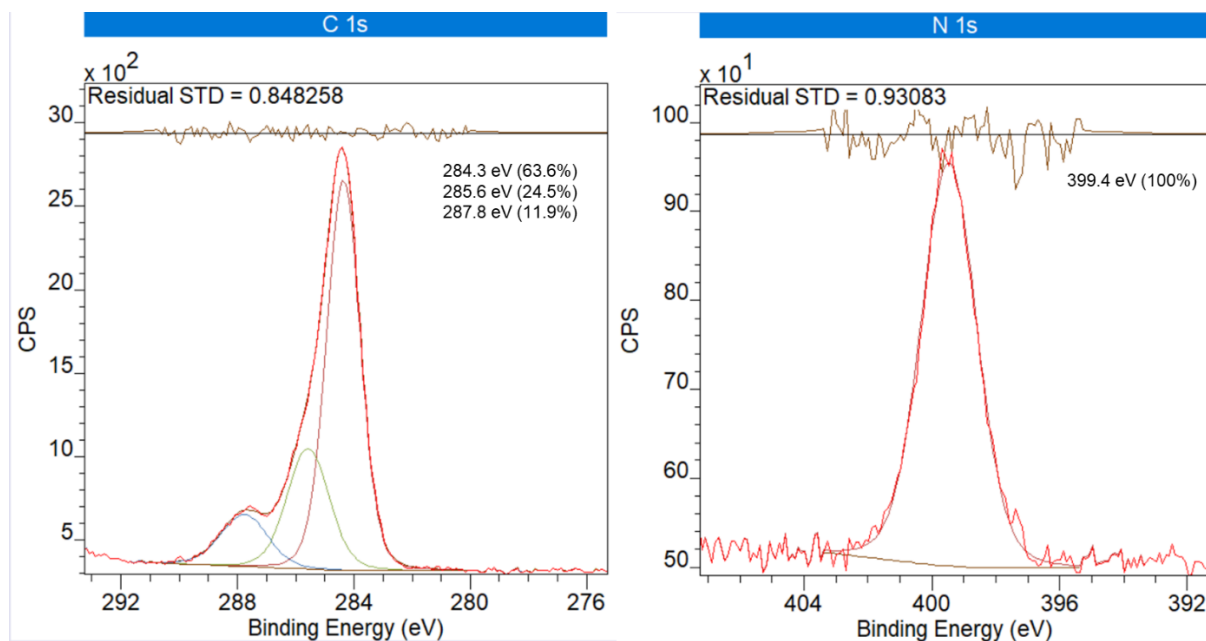


Figure S14. High-Resolution XPS spectra of GW@AQ.

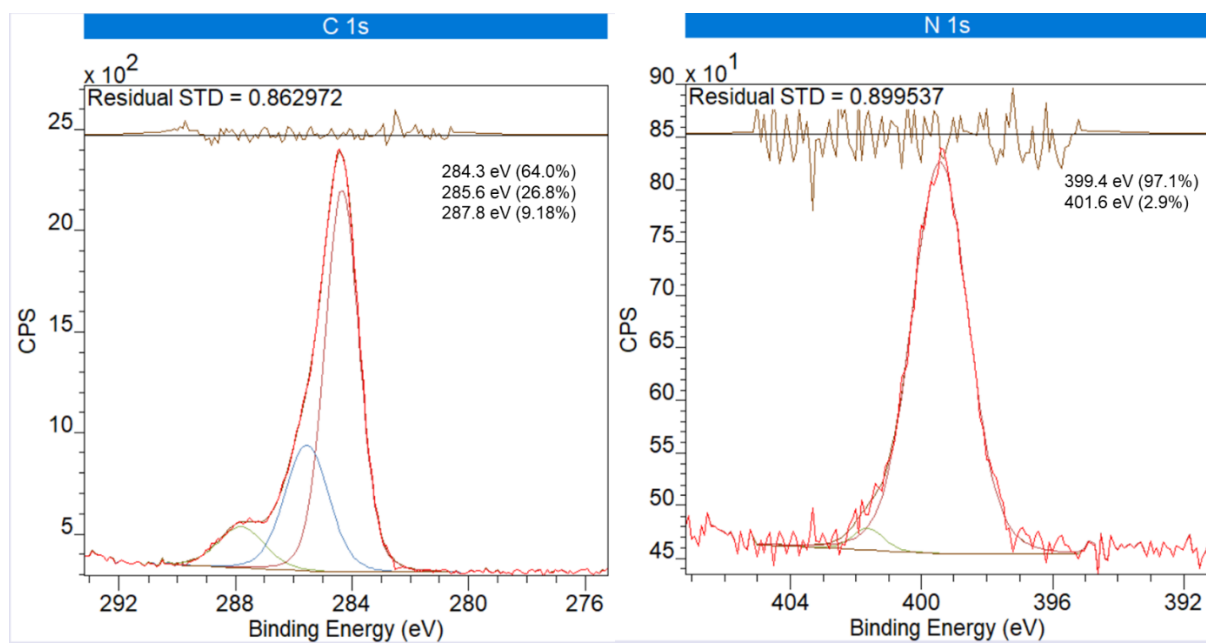


Figure S15. High-Resolution XPS spectra of GW@RB.

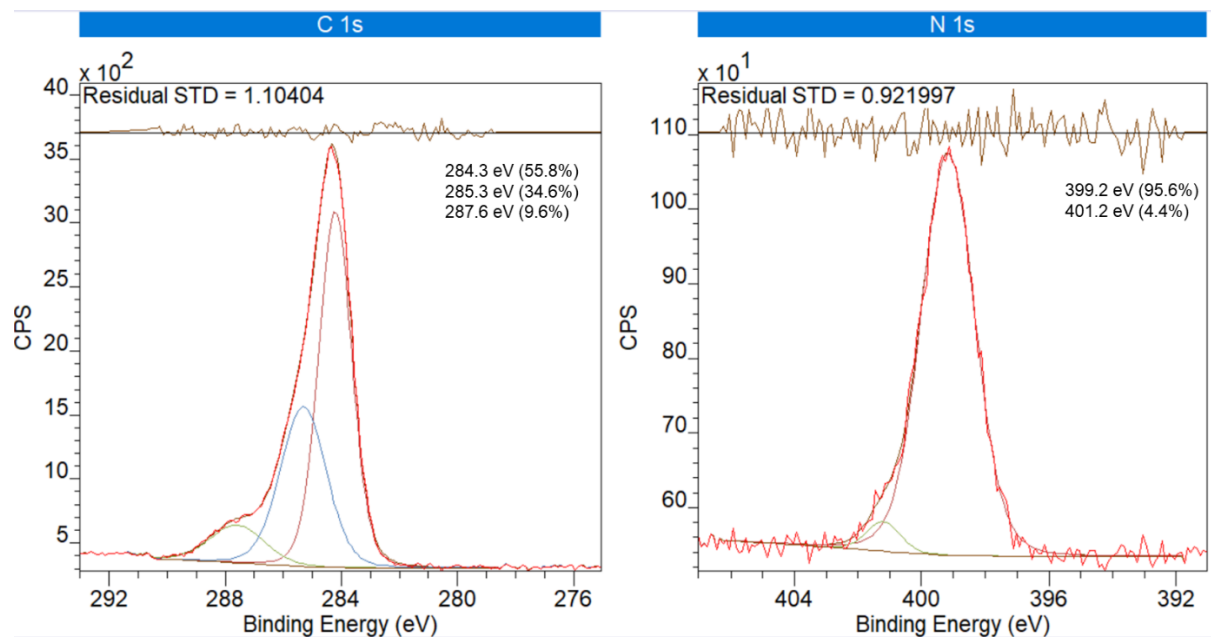


Figure S16. High-Resolution XPS spectra of GW@EY.

# NMR Spectroscopy

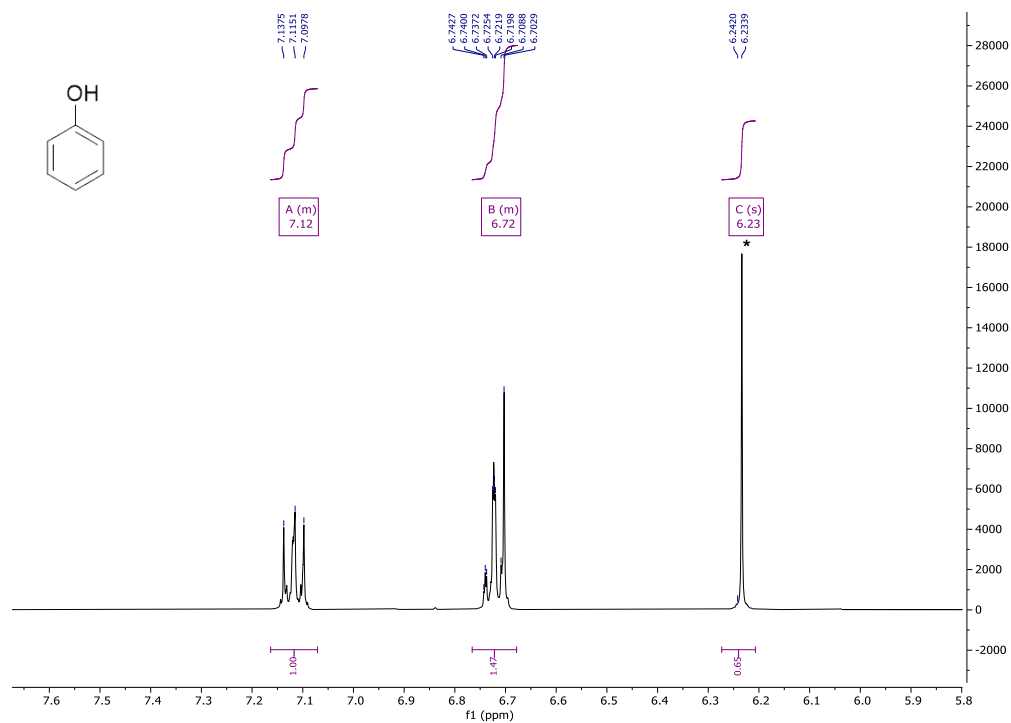


Figure S17. <sup>1</sup>H NMR spectrum of phenol obtained by oxidative hydroxylation of phenylboronic acid.  
\*maleic acid (7.4 mg).

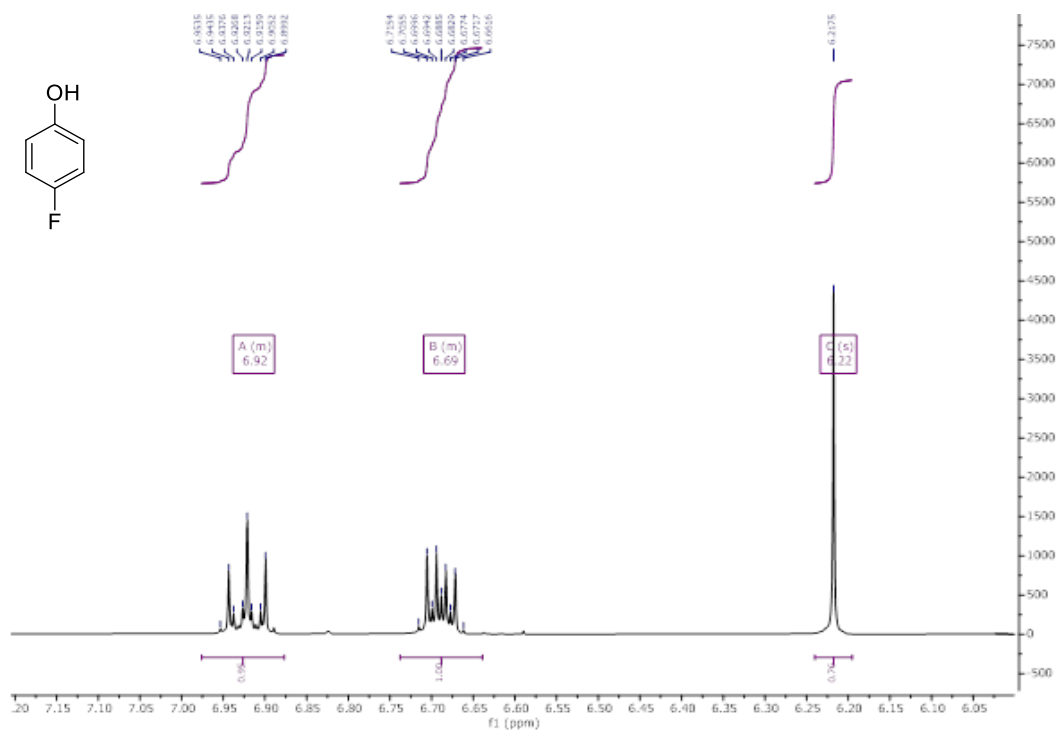


Figure S18.  $^1\text{H}$  NMR spectrum of 4-fluorophenol obtained by oxidative hydroxylation of 4-fluorophenylboronic acid. \*maleic acid (9.3 mg).

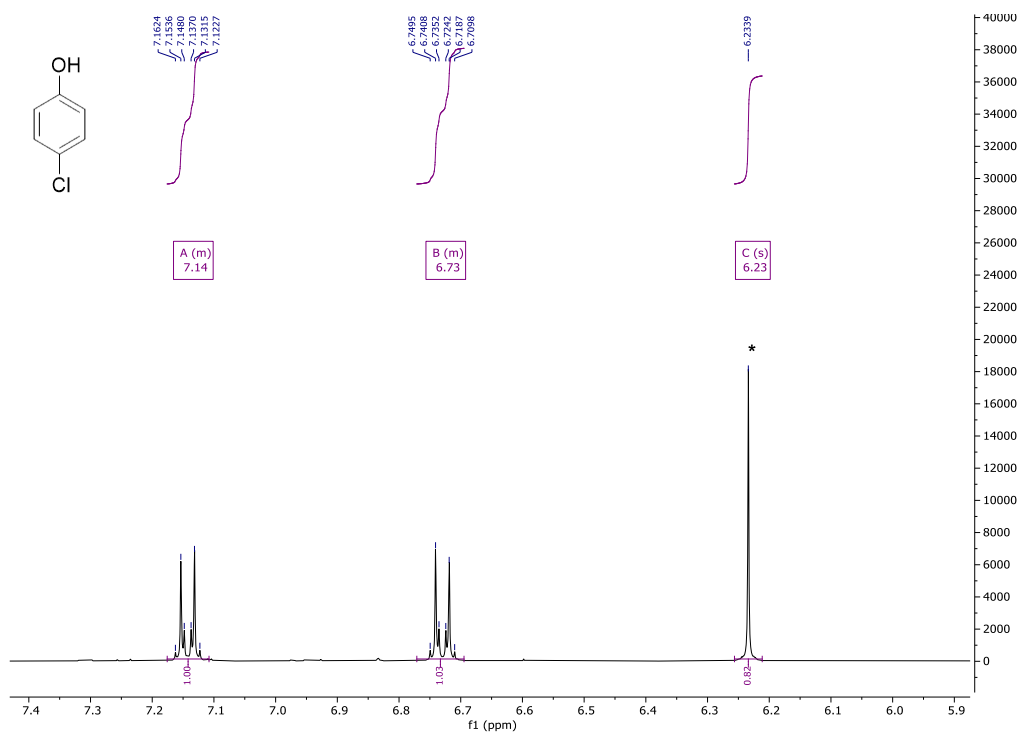


Figure S19.  $^1\text{H}$  NMR spectrum of 4-chlorophenol obtained by oxidative hydroxylation of 4-chlorophenylboronic acid. \*maleic acid (9.2 mg).

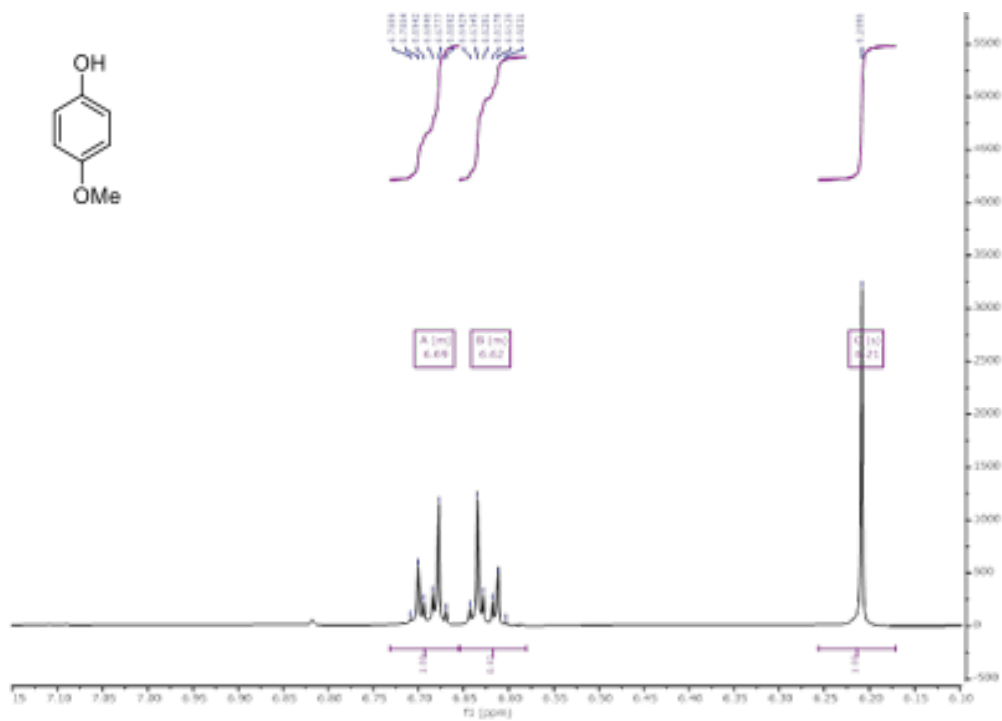


Figure S20.  $^1\text{H}$  NMR spectrum of 4-methoxyphenol obtained by oxidative hydroxylation of 4-methoxy phenylboronic acid. \*maleic acid (10.2 mg).

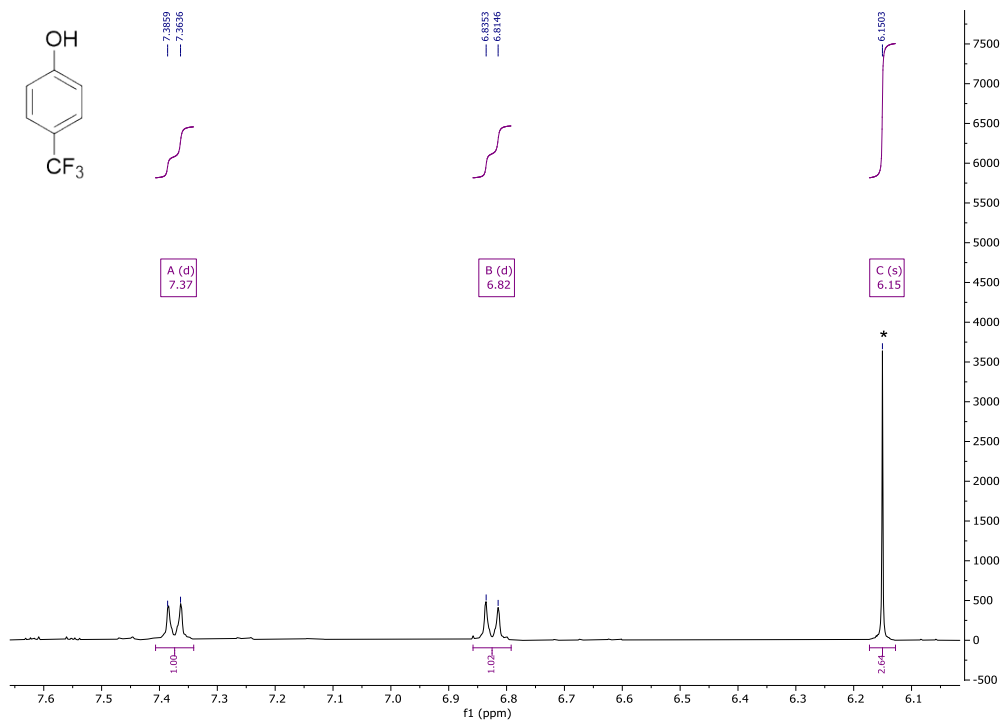


Figure S21.  $^1\text{H}$  NMR spectrum of 4-(trifluoromethyl)phenol obtained by oxidative hydroxylation of 4-(trifluoromethyl)phenylboronic acid. \*maleic acid (36 mg).

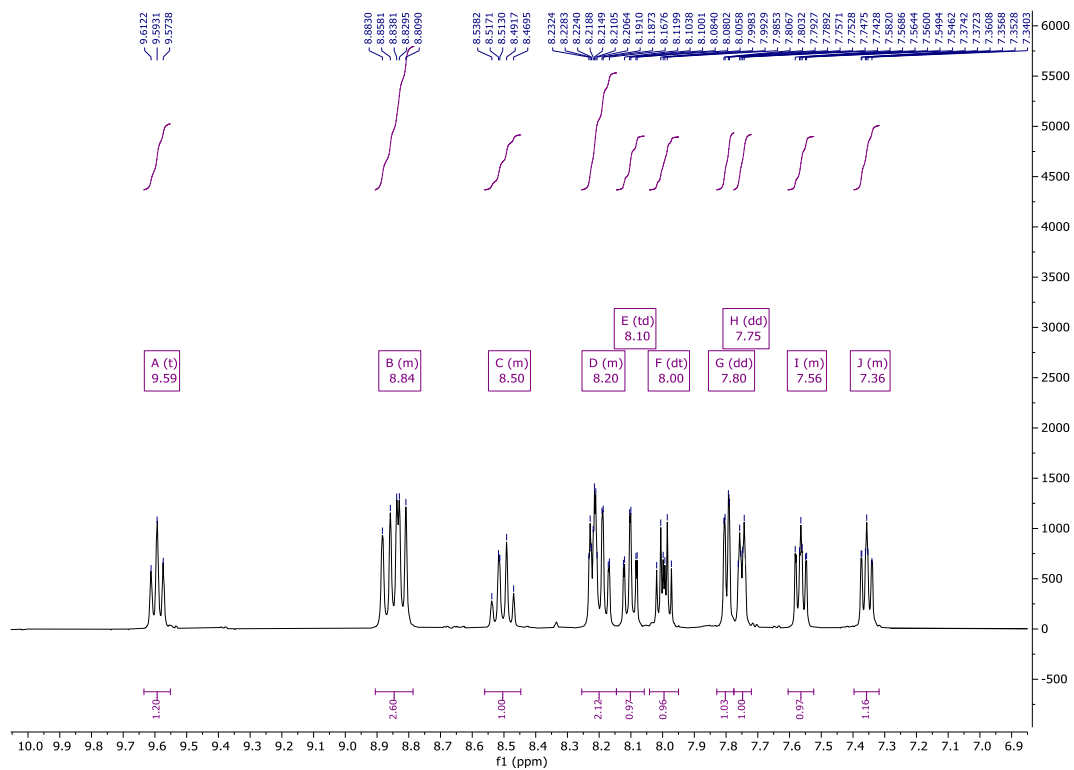


Figure S22.  $^1\text{H}$  NMR spectrum of RuB.

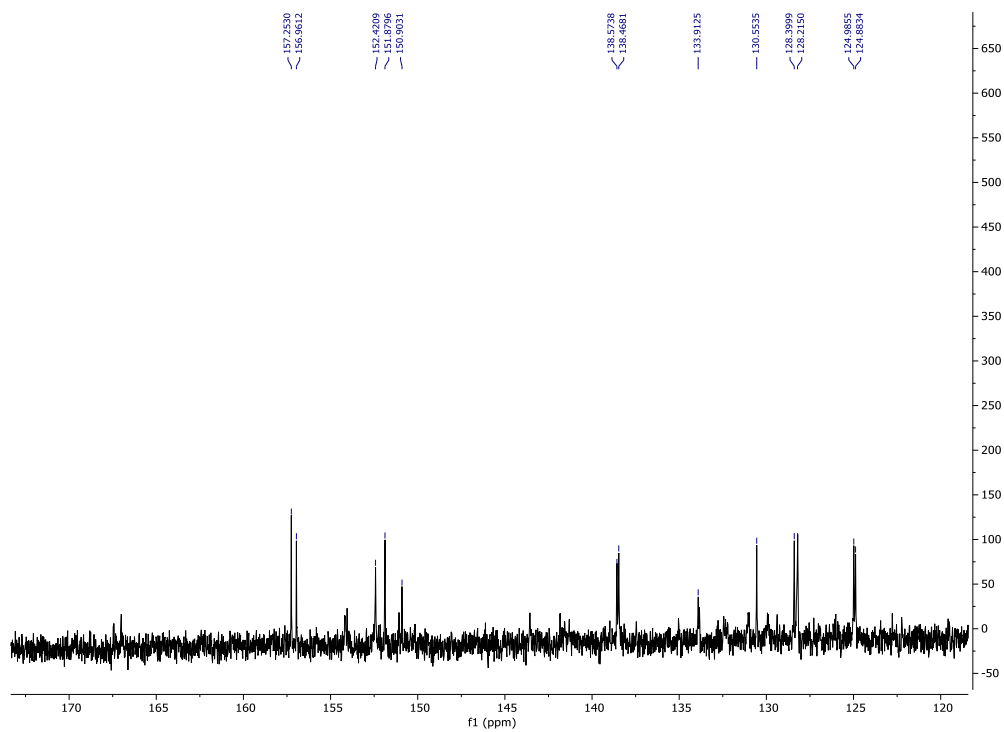


Figure S23.  $^{13}\text{C}$  NMR spectrum of RuB.

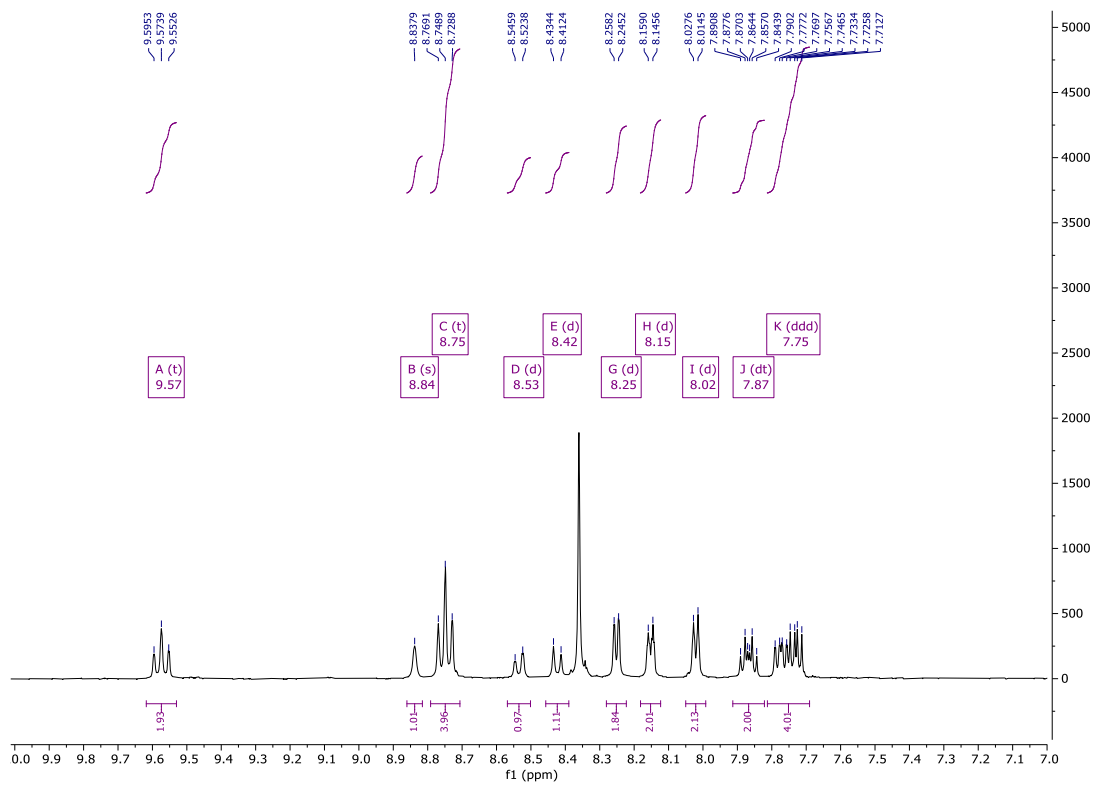


Figure S24. <sup>1</sup>H NMR spectrum of RuP.

ESI-HRMS

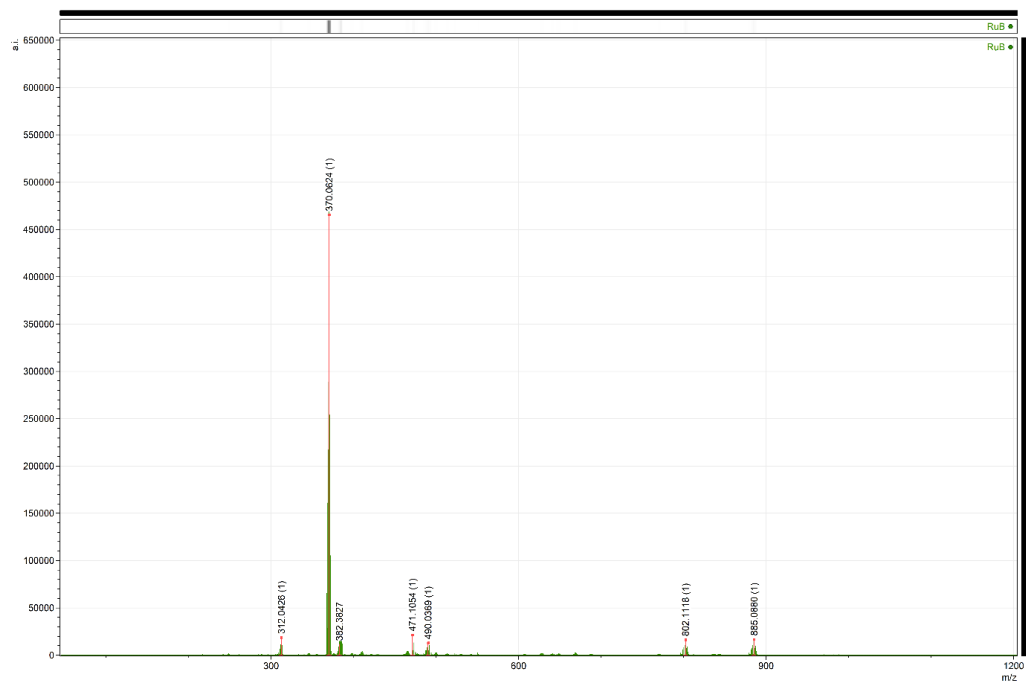


Figure S25. ESI-HRMS of RuB.

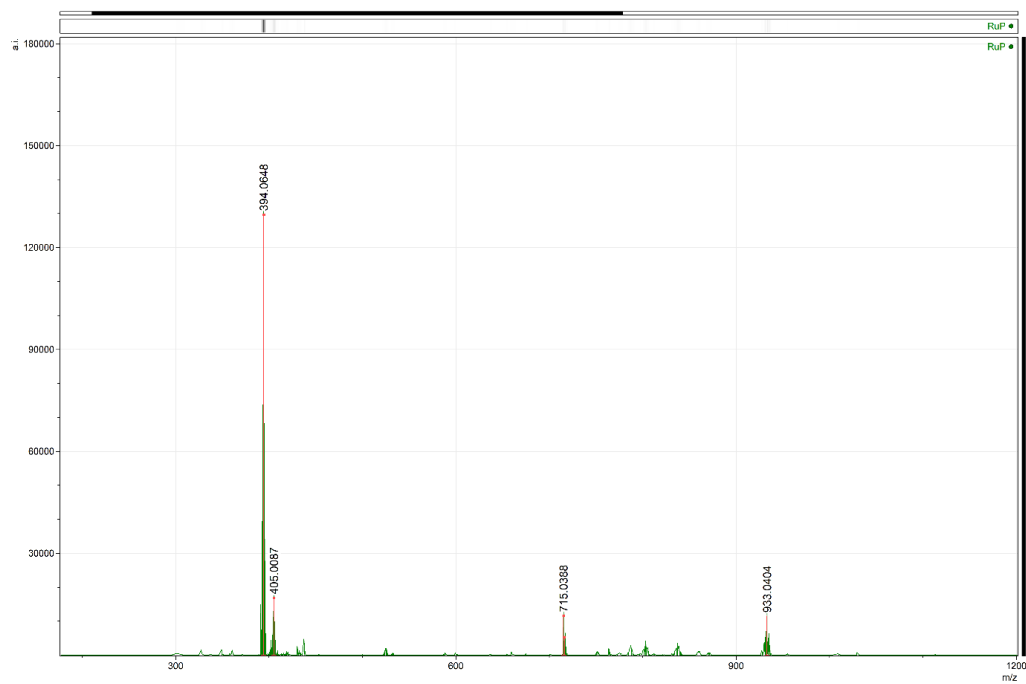


Figure S26. ESI-HRMS of RuP.

## Additional Results

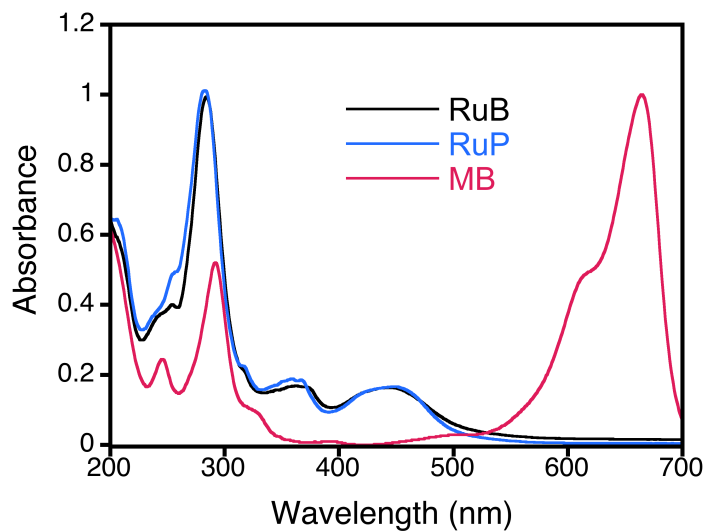


Figure S27. Absorption spectra of Ru-complexes versus MB.

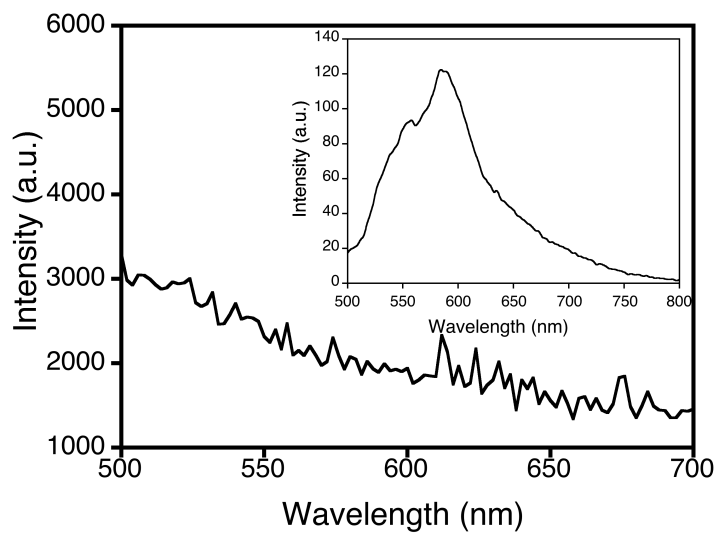


Figure S28. Emission spectrum of the reaction mixture of the hydroxylation of phenylboronic acid 6h after irradiation (blue LED) using GW@RuB as catalyst. Notice there is no evidence of RuB leaching during reaction (cft. inset: Emission spectrum of GW@RuB).

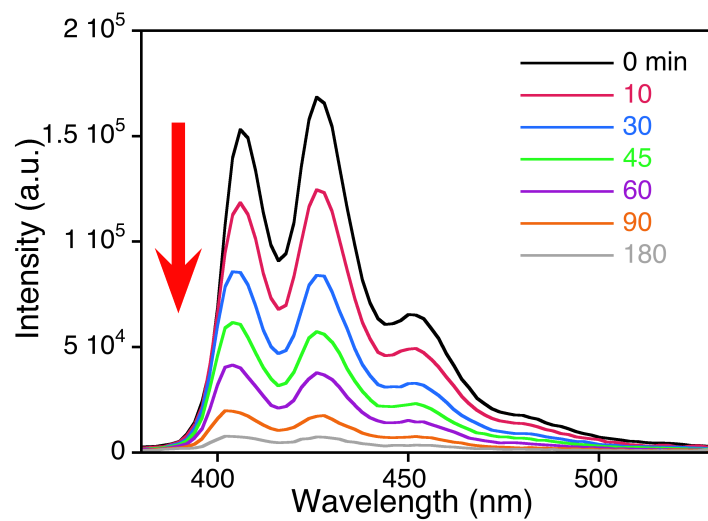


Figure S29. Kinetics of the photooxidation of a 100 μM DMA solution using GW@RuB as catalyst. Solvent: MeCN.

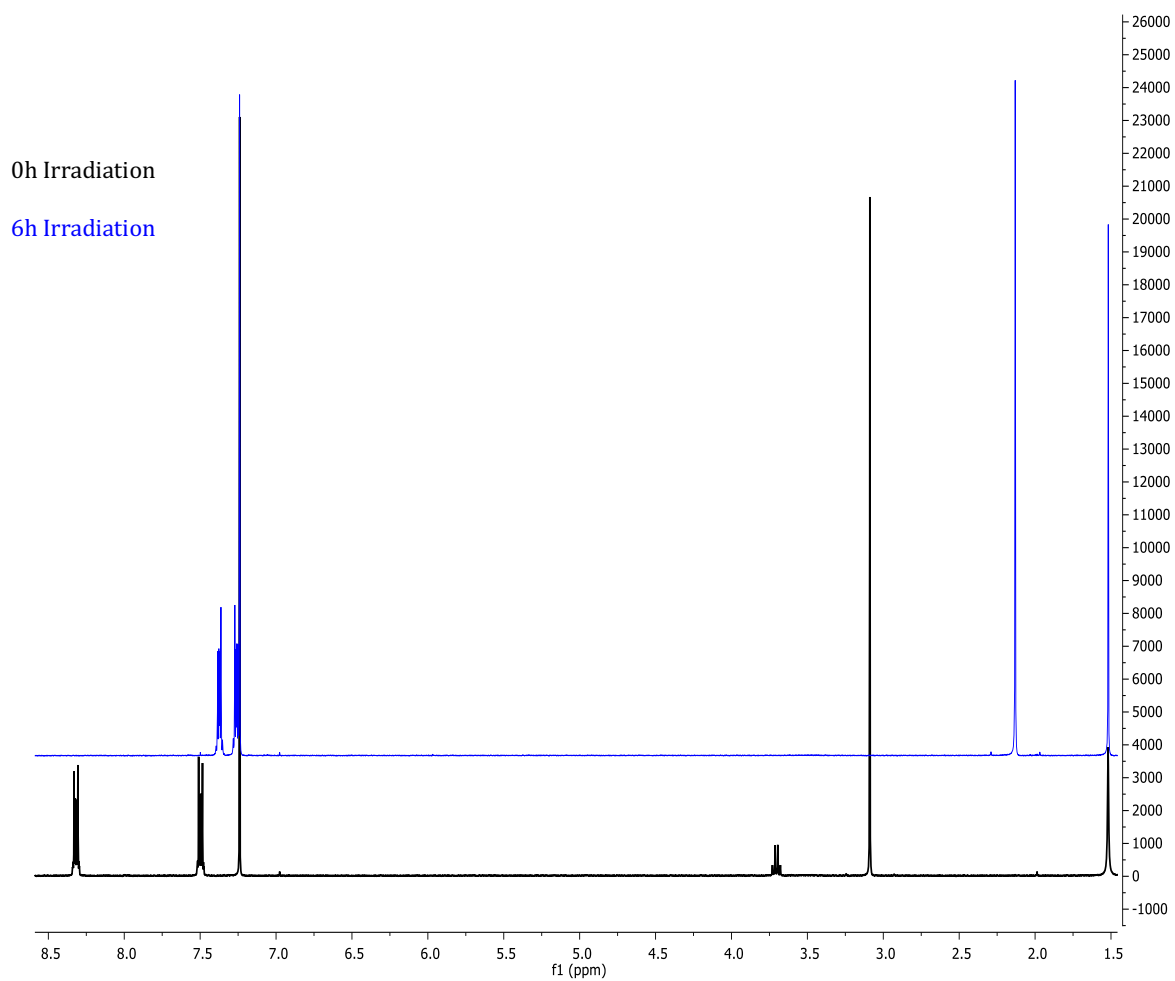


Figure S30. <sup>1</sup>H NMR spectra of DMA before (black) and after 6 h of (blue) blue LED irradiation using GW@RuB.

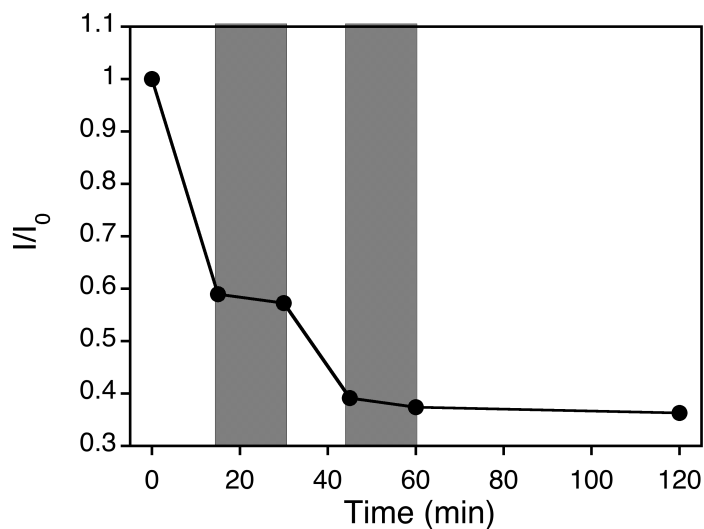


Figure S31. Decay of the DMA emission intensity versus time of irradiation (Blue LED) using GW@RuB as catalyst. General Procedure: 15 min irradiation of 5 mL of a DMA solution in the presence of 5 mg of GW@RuB. Filtration to remove the catalyst and further 15 min irradiation of the solution (grey area). Resubmission of catalyst into the solution and another 15 min irradiation cycle. Notice negligible conversion when the catalyst is taken out of the solution.

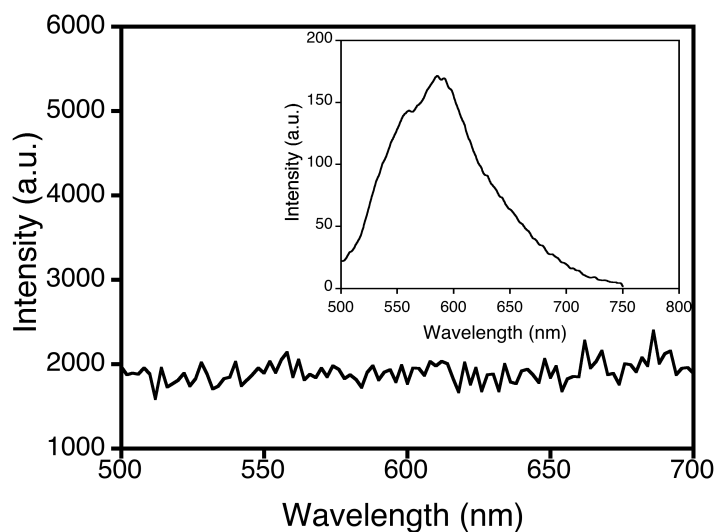


Figure S32. Emission spectrum of the reaction mixture of DMA oxidation after 2 h of blue LED irradiation using GW@RuP as catalyst. Notice there is no evidence of RuB leaching during reaction (*cf.* inset: Emission spectrum of GW@RuP).

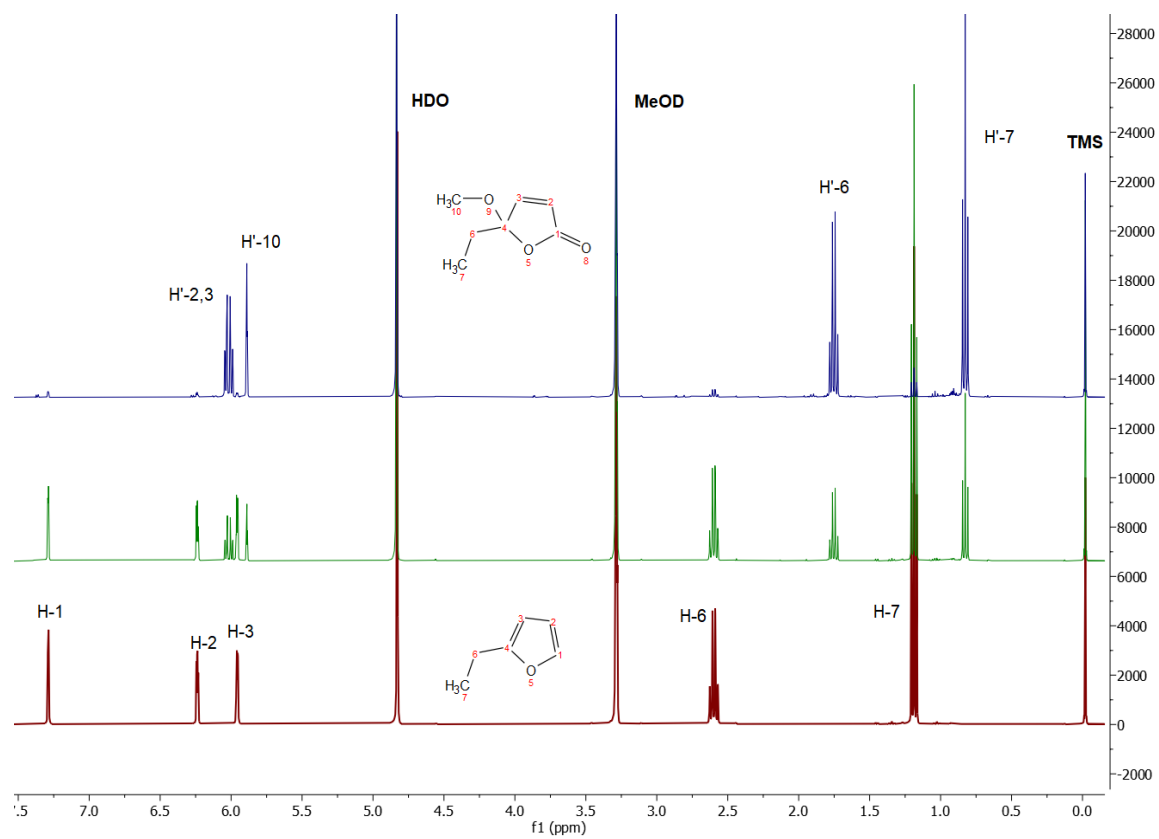


Figure S33. <sup>1</sup>H NMR spectra of 2-ethylfuran before (red), and after 3h (green) or 6h (blue) of blue LED irradiation using GW@RuB as catalyst.

## Excitation Sources

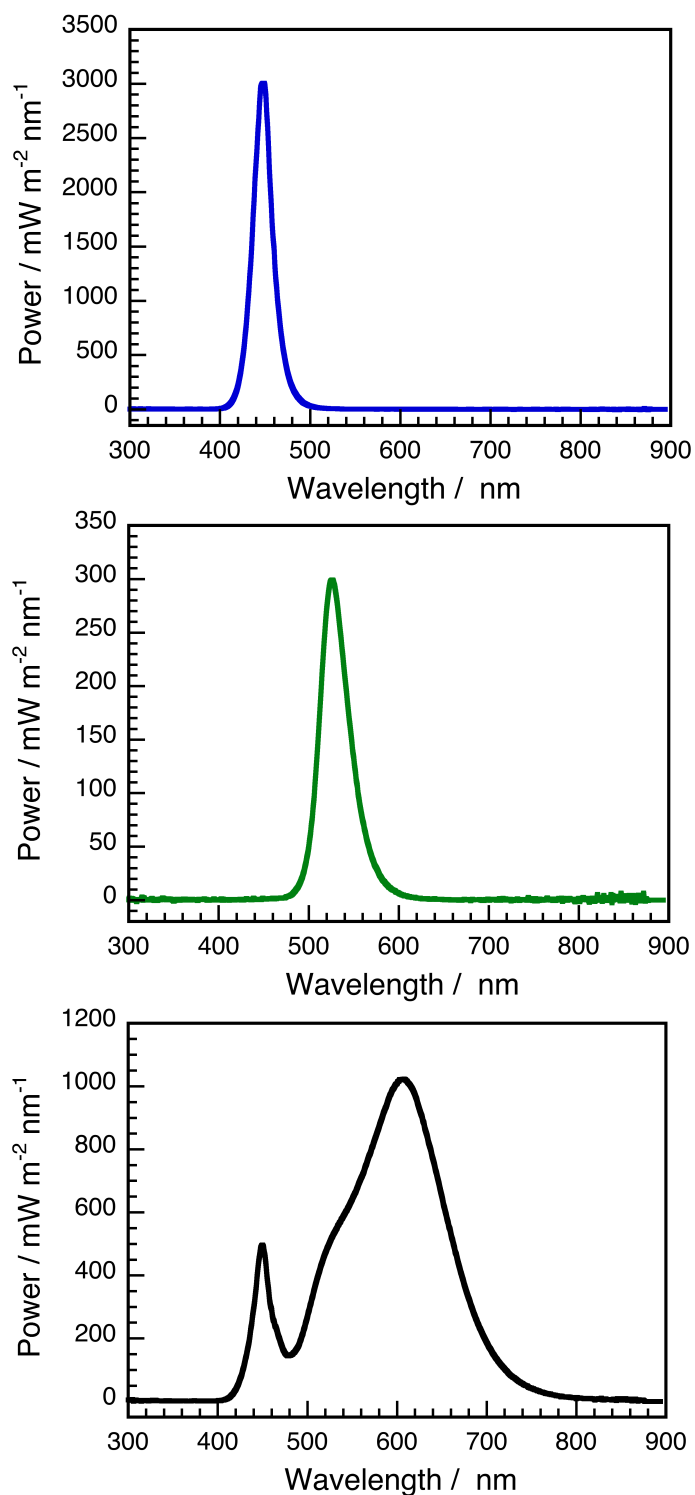


Figure S34. Emission spectra of (*top*) blue LED –working intensity: 1235 W/m<sup>2</sup>; (*middle*) green LED – working intensity: 855 W/m<sup>2</sup>; (*bottom*) white light LED –working intensity: 2385 W/m<sup>2</sup>.